Bathymetry of Mariana trench-arc system and formation of the Challenger Deep as a consequence of weak plate coupling

Zohar Gvirtzman

Geological Survey of Israel, Jerusalem, Israel

Robert J. Stern

Geosciences Department, University of Texas at Dallas, Richardson, Texas, USA

Received 9 September 2003; revised 20 January 2004; accepted 10 February 2004; published 2 April 2004.

[1] The Challenger Deep in the southernmost Mariana Trench (western Pacific Ocean) is the deepest point on the Earth's surface (10,920 m below sea level). Its location within a subduction trench, where one plate bends and descends below another, is not surprising. However, why is it located in the southernmost Mariana Trench and not at its central part, where the rate of subduction is higher, where the lithosphere is the oldest (and densest) on the Earth, and where the subducted lithosphere pulling down is the longest in the Earth (~1000 km or more according to seismic tomography)? We suggest that although subduction rate and slab age generally control trench depth, the width of the plate-coupling zone is more important. Beneath the central Marianas the subducted slab is attached to the upper plate along a 150-km-wide surface that holds the shallow portion of the subducted plate nearly horizontal, in spite of its great load and, thus, counters trench deepening. In contrast, along the south Mariana Trench the subducted length of the lithosphere is much shorter, but its attachment to the upper plate is only along a relatively narrow, 50-km-wide, surface. In addition, a tear in the slab beneath this region helps it to sink rapidly through the mantle, and this combination of circumstances allows the slab to steepen and form the deepest trench on the Earth. In a wider perspective, the interrelations shown here between trench deepening, ridge shallowing, slab steepening, and forearc narrowing may shed light on other subduction zones located near edges of rapidly steepening slabs. *INDEX TERMS:* 3045 Marine Geology and Geophysics: Seafloor morphology and bottom photography; 7218 Seismology: Lithosphere and upper mantle; 8120 Tectonophysics: Dynamics of lithosphere and mantle—general; 8122 Tectonophysics: Dynamics, gravity and tectonics; 8155 Tectonophysics: Plate motions—general; *KEYWORDS:* Mariana, Challenger Deep, plate coupling, residual topography, slab rollback, slab edge. **Citation:** Gvirtzman, Z., and R. J. Stern (2004), Bathymetry of Mariana trench-arc system and formation of the Challenger Deep as a consequence of weak plate coupling, *Tectonics*, *23*, TC2011, doi:10.1029/2003TC001581.

0278-7407/04/2003TC001581$12.00

1. Introduction

[2] The classic trench/arc/back arc geomorphology, so typical of the Mariana convergent plate boundary, changes markedly toward its southern end. The forearc narrows southward and the trench-arc distance decreases until the Mariana Ridge almost intersects the Mariana Trench near the island of Guam (Figure 1a). The southernmost Mariana Trench - referred to here as the Challenger Deep segment - trends nearly E-W in contrast to the more N-S orientation of most of the arc-trench system to the north. In addition, the westward-dipping Wadati-Benioff zone of earthquakes that is traced down to a depth of 600–700 km beneath the central Marianas can only be traced to a depth of about 200 km south of 16°N (Figure 1b).

[3] These unusual characteristics of the Challenger Deep segment (depth, trend, and seismicity) have led several investigators to conclude that this segment is a transform plate boundary [*Fujioka et al.*, 2002; *Karig and Rankin*, 1983]. On the other hand, the Pacific plate-Philippine Sea plate pole of rotation lies near the southern Marianas at about 8°N, 137.3°E [*Seno et al.*, 1993], so that relative plate motion in the Challenger Deep region is characterized by slow and slightly oblique convergence (Figure 1c).

[4] We show that seismicity beneath this region is best explained by the presence of a short (~200 km) subducted slab. The cluster of upper plate seamounts immediately north of the Challenger Deep segment (at about 142.5°E, 11.8°N), which appears to be the southward continuation of the magmatic arc [*Fryer*, 1996; *Fryer et al.*, 1998; *Martinez et al.*, 2000], support this interpretation.

[5] Nevertheless, recognizing that the Challenger Deep segment is a convergent rather than a transform plate boundary, begs the question as to why the world's deepest trench is associated with a relatively short (~200 km) slab at a point where the convergence rate is relatively slow (~2 cm/yr). This paper argues that although subduction rate and slab age generally control trench depth

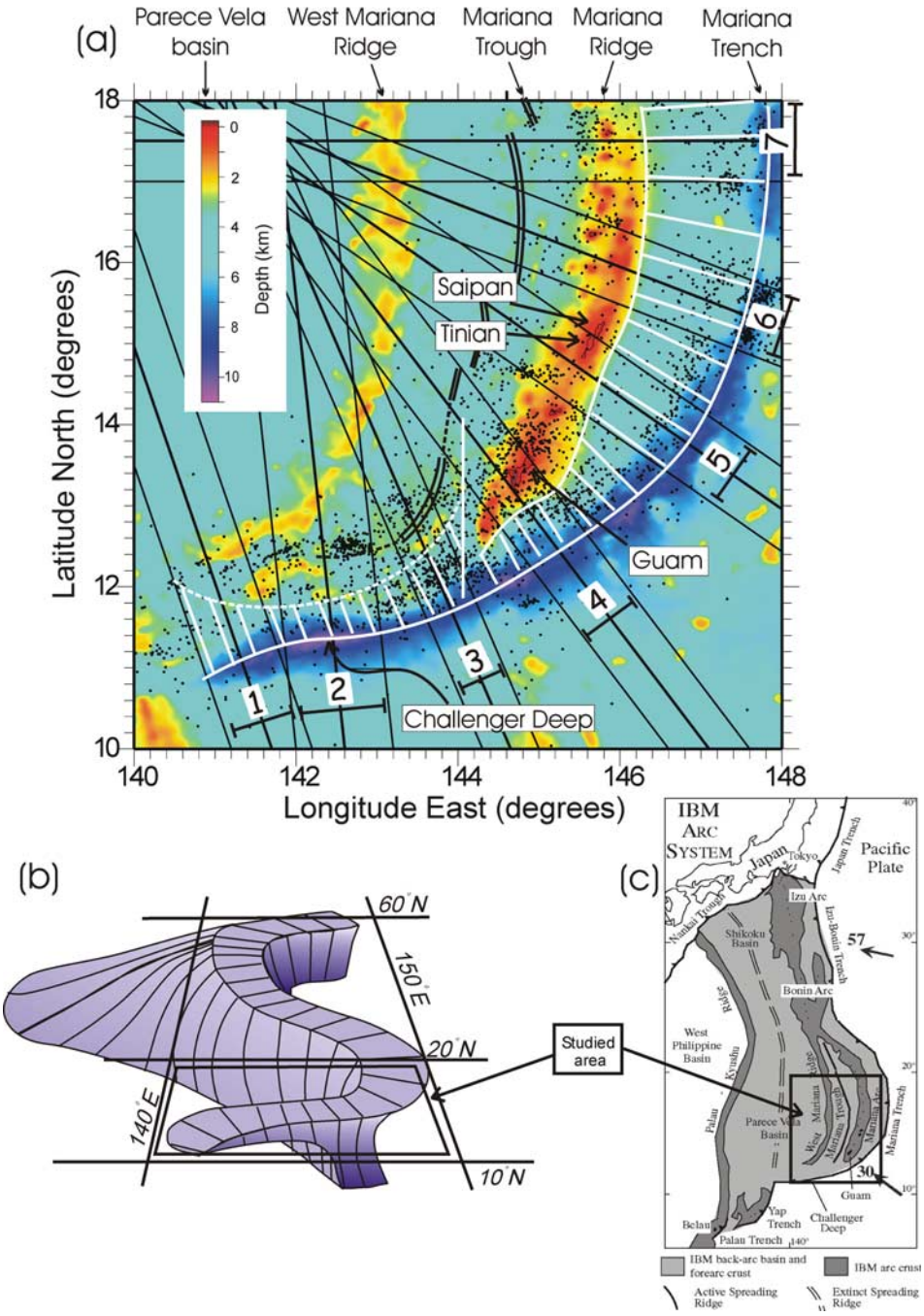

Figure 1. (a) Map showing bathymetry, principal tectonic elements, earthquake epicenters (black dots taken from the catalog of the National Earthquake Information Center, U.S. Geological Survey) and locations of seven sections across the Mariana subduction zone. Each section is marked by three parallel lines producing a ~100-km-wide band. Earthquakes within each band were projected onto a vertical central plane (the midline) to construct a structural cross section. The seven sections are presented in Figure 3. The hypocenters of sections 3 and 4 are shown in more detail in Figure 8. Note the north-south narrowing of the coupling zone (marked by thin white lines) extending from the trench axis to the eastern slopes of Mariana Ridge. Location of a proposed slab tear is marked by a thick white line. Location of the Mariana Trough spreading axis from *Martinez et al.* [2000]. (b) Cartoon illustrating the geometry of the subducting Pacific plate under the entire Mariana-Japan-Kurile arc system (drawn after *Gudmundsson and Sambridge* [1998]). Note the dramatic shortening of the slab at the southern edge of the Marianas. (c) A general tectonic map of the Philippine Sea region. Thick arrows show the relative motion of the Pacific plate with respect to the Philippine Sea plate. Numbers correspond to velocities (mm/year) [after *Seno et al.*, 1993].

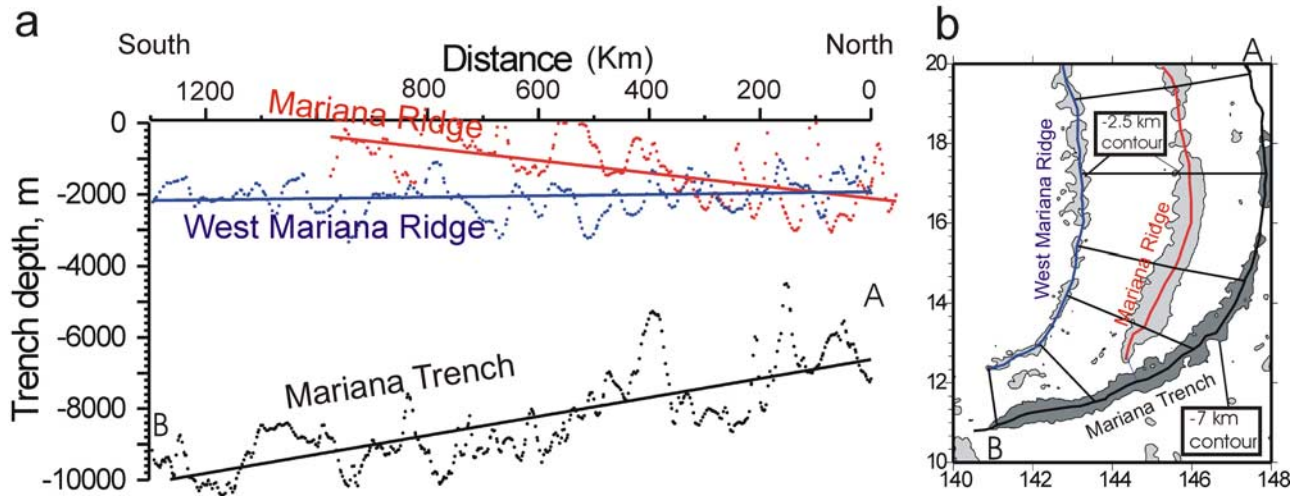

Figure 2. (a) Topography along the axes of the Mariana Trench, Mariana Ridge, and West Mariana Ridge. Ridge axes were stretched to fit trench axis controlled by six tie points shown in Figure 2b. Complementary trends observed along the Mariana Ridge and Trench suggests that plate coupling weakens southward. This allows the subducting plate to sink more freely in the mantle and steepen and at the same time allows the free overriding plate to rise and rebound. Note that short-wavelength variations are observed along both ridges, whereas a regional trend is observed only along the southernmost Mariana Ridge. This observation supports the interpretation that the regional trend along the Mariana Ridge is related to plate boundary activity in contrast with the short wavelength variations probably reflecting local changes in crustal thickness that are observed along both ridges.

[*Grellet and Dubois*, 1982; *Jarrard*, 1986], here in the southern Mariana Trench, the width of the plate-coupling zone is more important. We suggest that the unusual depth of the Challenger Deep is related to an exceptionally narrow plate-coupling zone, where the heavy descending slab hangs almost entirely on the oceanic plate with a very weak attachment to the upper plate. As a result of the weak coupling, the descending oceanic plate is relatively free to sink and steepen, resulting in an unusually deep trench, whereas the upper plate, released from the heavy slab, rebounds and forms a relatively shallow ridge. This interpretation is consistent with *Fryer et al.* [2003], who interpret the normal faulting in the forearc as extension due to rapid slab rollback (see discussion).

2. Observations

2.1. Bathymetry

[6] The southern Mariana region is one of the roughest surfaces on the Earth's skin, especially in the vicinity of the Challenger Deep where relief reaches about 9 km within a short distance of about 60 km. However, examining the bathymetric variations along the axis of the Mariana Trench suggests that the Challenger Deep is not just another local disturbance in the bathymetry. Rather, it is a part of a regional topographic trend of deepening that extends along a distance of more than 1000 km and accumulates to more than 3 km in depth. Figure 2 shows this trend (solid black line) superimposed on the steeper, short-wavelength (100–200 km) variations in the bathymetry. Figure 2 further shows that an opposite trend of gradual shallowing southward by ~2 km is evident along the adjacent Mariana Ridge (red solid line).

2.2. Seismicity

[7] To further examine lateral variations along the Mariana plate boundary we examine the Wadati-Benioff zone using the earthquake catalog of the U.S. Geological Survey (National Earthquake Information Center, NEIC). Figure 3 shows seven cross sections, each marked on the map of Figure 1a by three parallel lines that produce a ~100-km-wide band. Earthquakes within each band were projected onto a vertical central plane (the midline) to construct a structural cross section portraying the shape of the subducting Pacific plate. Two dashed lines along the seismogenic zone illustrate the uncertainty in determining the exact location of the top of the plate. This uncertainty reduces toward the surface, where the two lines meet at the trench axis.

[8] In sections 3–4 hypocenters are distributed over a region thicker than a reasonable plate. This may indicate that these sections are crossing the subducting plate diagonally or that some other disruption occurs (see discussion in section 5.3 and Figure 8). In any case the shape of the subducting plate cannot be portrayed on these sections. However, in spite of the inability to determine the shape of the subducting plate in sections 3–4 and in spite of the range of uncertainties in the other sections, the difference between central and

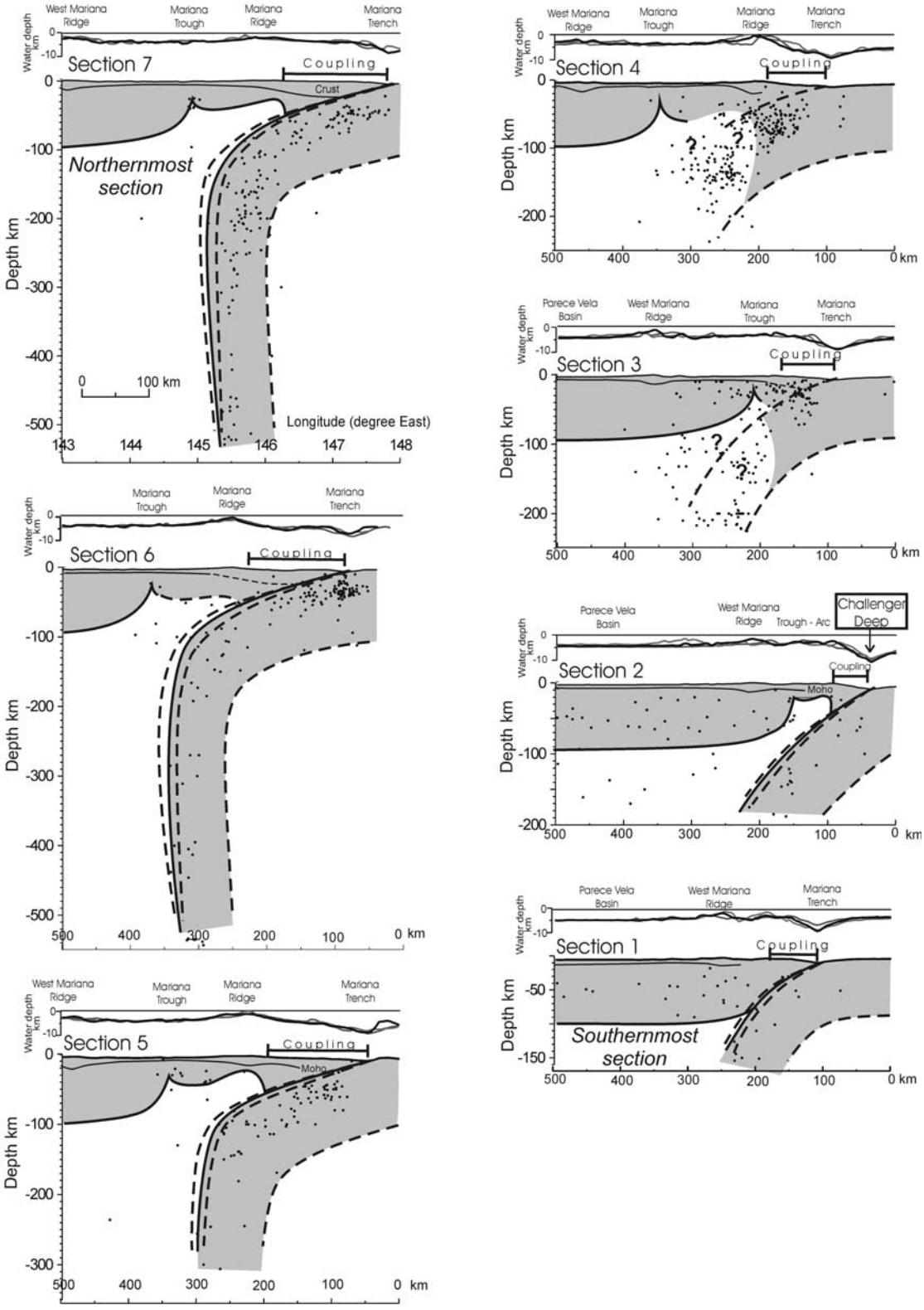
West Mariana Ridge
Mariana Trough
Mariana Ridge
Mariana Trench
Water depth km
Section 7
Coupling
Crust
Northernmost section
Depth km
0 100 km
Longitude (degree East)
143 144 145 146 147 148
Section 6
Section 5
Moho
Section 4
Parece Vela Basin
Section 3
Challenger Deep
Trough - Arc
Section 2
Section 1
Southernmost section
0 km

Figure 3.

southern Marianas is most evident. Beneath the central Marianas (sections 6 and 7) the subducting plate strongly bends to nearly vertical, but it first dips quite gently (~16°–17°). In contrast, beneath the southern Marianas (sections 1, 2) the subducting slab is only traced by earthquakes to a depth of 150–200 km, but its dip in that depth range is much steeper (~29°–34°).

3. Hypothesis: Southward Weakening of Plate Coupling

[9] The opposite topographic trends of the Mariana Trench and the Mariana Ridge on the two sides of the Mariana plate boundary (Figure 2) beg for a plate boundary explanation, especially in light of the absence of any topographic trend along the West Mariana Ridge (blue line), which is a few hundred kilometers away from the plate boundary. We hypothesize that the short-wavelength variations in elevation observed for both ridges reflect local changes in crustal thickness, whereas the regional topographic trends approaching the plate boundary reflect a regional tectonic process.

[10] In what follows we establish this hypothesis by showing that the zone of coupling between the plates narrows southward and that the asthenosphere propagates upward between the downgoing and overriding plates. This, we suggest, weakens the coupling between the plates allowing the subducting plate to steepen (in the upper 50–100 km) and form a deeper trench and at the same time allows the edge of the overriding plate to be released from the descending slab and rebound, accounting for the southward increase in elevation of the Mariana Ridge.

[11] Using the term "plate coupling" here, we refer to the resistance of the plates to detach vertically as expressed by the down-pulling action on the upper plate by the descending plate (Figure 4). It is important to understand that this meaning of coupling differs from "seismic coupling" [*Pacheco et al.*, 1993; *Peterson and Seno*, 1984; *Ruff and Kanamori*, 1980; *Scholz and Campos*, 1995] that refers to the resistance of the plates to slip against each other as expressed by occasional strong interplate thrust earthquakes. Although "shear coupling" and "pull-down coupling" must be related, because both refer to the lithosphere-lithosphere contact along the subduction interface, here we focus only on the vertical detachment forces in order to show its influence on the topography of the trench-arc system.

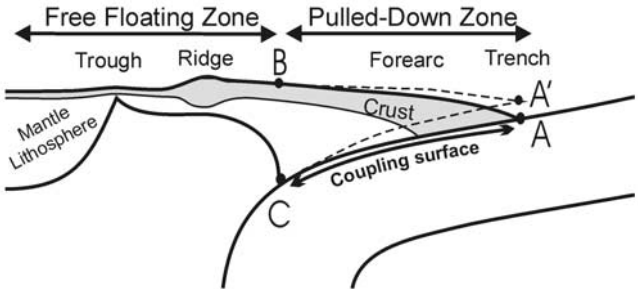

Figure 4. An illustration of vertical plate coupling. The leading edge of the overriding plate (triangle ABC) coupled to the subducting slab is bent and pulled down to a position lower than expected for isostatic equilibrium of a free plate edge (triangle A′BC). B is the transition point, where observed topography suits the buoyancy of a free overriding plate. The region from B trenchward is considered as the Pulled-Down Zone, where topography is lower than expected from local lithospheric buoyancy. The region from B arcward is considered as the Free Floating Zone, where the overriding plate is no longer pulled down and maintains isostatic equilibrium.

4. Analysis

4.1. Down-Pulled Zone Versus Free Floating Zone

[12] Consistent with our definition of plate coupling, we identify the boundaries of the coupling zone by determining where the overriding plate is significantly lower than

Figure 3. Inferred lithospheric sections (locations in Figure 1) showing the top of the subducting plate, the base of the overriding plate, and the coupling surface where these two lines meet. The top of the subducting plate is approximated from earthquake distributions taken from the catalog of the U.S. Geological Survey (National Earthquake Information Center, NEIC). Crustal earthquakes with no accurate specification of depth were not included. Two dashed lines show the range of uncertainty in determining the top of the plate. Note that this uncertainty is quite small at the upper 50 km, where we measure slab dip for further analysis (in Figure 6). The base of the overriding plate is inferred from topographic analysis [*Gvirtzman*, 2002; *Gvirtzman and Nur*, 1999a, 1999b, 2001] as illustrated in and explained in Appendix A. The idea is that considering the buoyancy of a given crust, the thickness of the mantle lithosphere can be calculated in a way that matches the total buoyancy of the lithosphere with the observed surface elevation. Crustal thicknesses used for this analysis are as follows: 5.5 km in the Parece Vela and Mariana Trough back arc basin [*Fryer and Hussong*, 1981; *Latraille and Hussong*, 1980]; 11 km under the Mariana Ridge at 18°N (section 7 [*Fryer and Hussong*, 1981]); 15 km under the Mariana Ridge at 14.5°N ([*Lange*, 1992; *Zhang and Langston*, 1995], section 5); 10 km in what seems as a developing arc in section 2 (this is an upper limit as explained in text); and 17 km under the West Mariana Ridge [*Bibee et al.*, 1979]. Above each section three detailed topographic sections are shown with vertical exaggerations of ~5 (thick line represents the midline of each band (shown on Figure 1a); thin lines represent topography along the bounding lines). Note the decrease of plate-coupling zone width from about 150 km in section 7 to approximately 50 km in section 2 (further shown in Figure 8a). The question marks in sections 3 and 4 express the unclear geometry of the subducting plate as seen by the wide scattering of hypocenters (these sections are furthered analyzed in Figure 8).

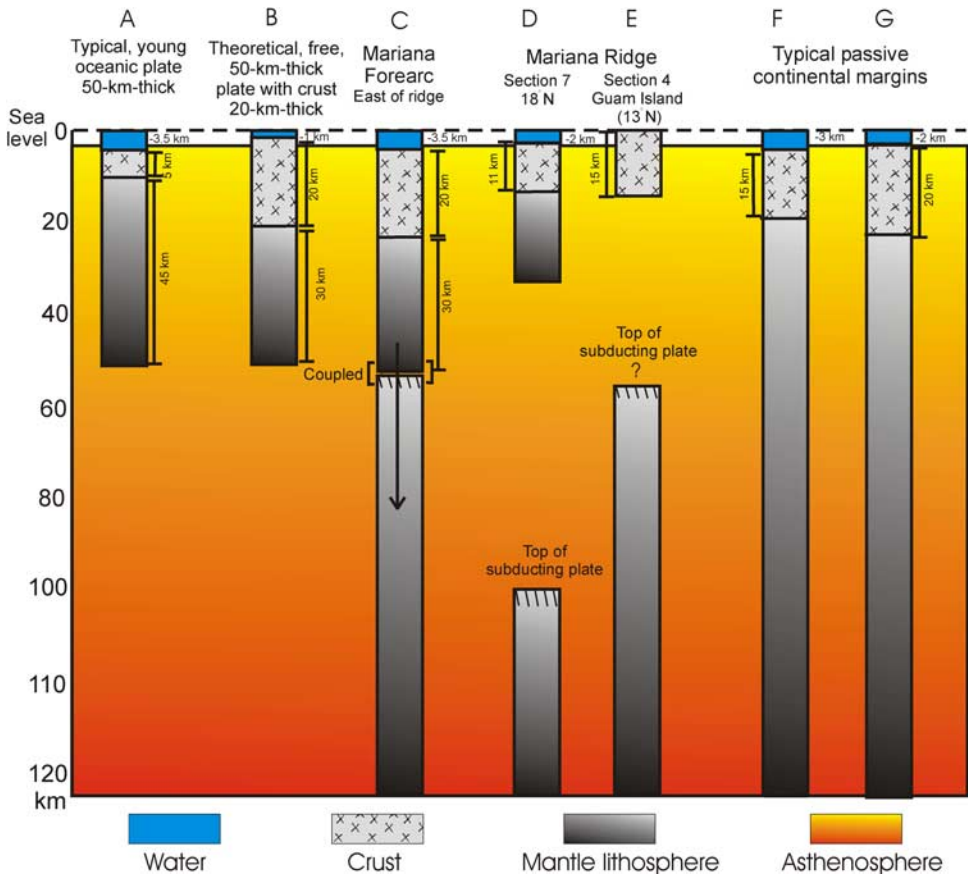

Figure 5. Cartoon illustrating the floating state of various lithospheric columns assuming that the lithosphere is sustained in a flowing asthenosphere (based on *Gvirtzman* [2002] and *Gvirtzman and Nur* [1999b] and on *Lachenbruch and Morgan* [1990]). Column A shows that in 3.5-km-deep ocean the crust is usually about 5-km thick and the entire lithosphere is about 50-km thick. For comparison, in the Mariana forearc east of the Mariana Ridge, similar water depths and plate thicknesses (i.e., from the surface to the Wadati-Benioff seismic zone) are associated with a crust that is about 4 times thicker (20 km at 18°N [*Fryer and Hussong*, 1981]). Column B further illustrates that, theoretically, in local isostatic equilibrium the surface of a free 50-km-thick plate with a 20-km-thick crust is expected to lie ~1 km below sea level [*Gvirtzman*, 2002; *Gvirtzman and Nur*, 1999b; *Lachenbruch and Morgan*, 1990] and not 3.5 km as observed. This suggests that the Mariana forearc is coupled to and pulled down by the underlying subducting plate. Column D describes the isostatic state of the Mariana Ridge at 18°N (central Marianas, section 7), where the crust is 11-km thick [*Fryer and Hussong*, 1981] and water depth is −2 km. Here, isostasy implies that the thickness of the mantle lithosphere should be 20 km [*Gvirtzman*, 2002; *Gvirtzman and Nur*, 1999b; *Lachenbruch and Morgan*, 1990] and thus the base of the lithosphere should be at a depth of about 31 km, nearly 70 km above the top of the subducting plate. We thus conclude that 70 km of asthenosphere lies between the two plates under the ridge and that the overriding plate is freed from the downgoing plate. Column E illustrates the southern Mariana Ridge, which is clearly too high compared with its crustal thickness. It is suggested that beneath Guam the crust directly overlies the asthenosphere without any mantle lithosphere, that is, without the heavy component of the plate. For comparison, column F shows that in passive continental margins a 15-km-thick crust is associated with water depths of about 3 km and not zero as in Guam; and column G shows that in passive continental margins a 20-km-thick crust is associated with water depths of 2 km and not −3.5 km as in Mariana forearc.

expected from local lithospheric buoyancy (Figure 4). It is relatively easy to show that the Mariana forearc (east of the Mariana Ridge) falls within this category. The thickness of the overriding plate under this region (down to the top of the Wadati-Benioff seismic zone) changes from zero at the trench to approximately 50 km under isobath −3.5 km. Figure 5a illustrates that the surface of a 50-km-thick oceanic plate with a typical ~5-km-thick crust should lie

3.5 km below sea level. However, beneath the Mariana forearc at 18°N (section 7 of Figure 3 and Figure A1 in Appendix A), crustal seismic velocities are identified down to a depth of at least 9 km [*Latraille and Hussong*, 1980] and the total thickness of the crust is estimated as 20 km [*Fryer and Hussong*, 1981]. Crust of this thickness should be associated with seafloor that is shallower than 3.5 km. In fact, isostatic considerations [*Gvirtzman and Nur*, 1999b; *Lachenbruch and Morgan*, 1990] predict that the surface of a free, 50-km-thick, plate with a 20-km-thick crust should lie ~1 km below sea level (Figure 5b) and not 3.5 km as observed for the Mariana forearc. Therefore we argue that the Mariana forearc is clearly within the coupling zone, where the tip of the overriding plate is attached to and pulled down by the subducting plate (Figure 5c); this interpretation is also consistent with the low heat flow characteristic of the forearc implying no subjacent asthenosphere.

[13] In contrast, the Mariana Ridge (sometimes referred to as the Mariana Frontal Arc) appears to be too high compared with its crustal thickness of only 11 km at 18°N [*Fryer and Hussong*, 1981]. To explain such thin crust with an average water depth of −2 km, isostasy requires that the thickness of the mantle lithosphere should be 20 km [*Gvirtzman and Nur*, 1999b; *Lachenbruch and Morgan*, 1990]; that is, a total plate thickness of ~31 km. Considering that the top of the subducting plate at this point is about 100-km deep (the top of the seismic zone), we conclude that 70 km of asthenosphere lies between the two plates below the ridge at 18°N (Figure 5d). The presence of asthenosphere between the lithospheres of the overriding and downgoing plates frees the overriding plate from being pulled down by the downgoing plate. The sharp break in water depth between the Mariana forearc and the Mariana Ridge (approximately isobath −2.5 km) thus approximates the trenchward limit of asthenosphere beneath the overriding plate.

[14] The circumstance of an anomalously elevated ridge is even more apparent in the south where the Mariana Ridge shallows and at some places pops out of the water. In this region, crustal thicknesses were estimated as 16 km near Saipan and Tinian (OBS study [*Lange*, 1992]) and 15 km under Guam (receiver function inversion [*Zhang and Langston*, 1995]). This combination of crustal thickness and elevation is indeed exceptional, because a 15–16-km-thick crust with a density of 2800–2850 kg/m^3 should be drowned a few hundred meters below sea level even if it directly overlies asthenosphere with no mantle lithosphere at all [*Gvirtzman and Nur*, 1999b; *Lachenbruch and Morgan*, 1990] (that is, even without the heavy component of the plate, Figure 5e). Therefore, we believe, a thickness of 15–16 km is a good average estimate of crustal thickness in the vicinity of the islands, whereas locally beneath the islands themselves the crust may be a bit thicker.

[15] Recognizing that the Mariana forearc is mostly within the Down-Pulled Zone and that the Mariana Ridge is in the Free Floating Zone (Figure 4), we argue that the southward narrowing of the forearc reflects the southward narrowing of the plate-coupling zone. Figure 3 shows this narrowing in cross sections. The coupling zone in all these sections extends from the trench axis to the sharp break in bathymetry at the eastern slope of the Mariana Ridge (approximately at isobath −2.5 km). So defined, the width of the coupling zone decreases from about 150 km along section 7 to only about 50 km for section 2.

4.2. Shape of the Asthenospheric Wedge Between Subducting and Overriding Plates

[16] In addition to the plate-coupling zone, the sections of Figure 3 also show the shape of the asthenospheric wedge between the subducting and overriding plates. The top of this wedge is inferred by mapping the base of the overriding plate using a topography-buoyancy analysis that is described in Appendix A. This analysis considers the buoyancy of a known or estimated thickness of crust and calculates the thickness of the underlying mantle lithosphere to match the total buoyancy of the lithosphere needed to produce the observed surface elevation [*Gvirtzman*, 2002; *Gvirtzman and Nur*, 1999a, 1999b, 2001]. The calculation is based on the assumption of isostatic equilibrium, which holds only in the zone of a free floating lithosphere, that is, west of the eastern slopes of the Mariana Ridge (see discussion). Also, we assume that isostasy is local in this region where the lithosphere is hot and weak and thus cannot support significant loads by its own strength. For a step by step illustration of this analysis see Appendix A and for further details about uncertainties related to this method see *Gvirtzman and Nur* [2001].

[17] Comparing the seven cross sections of Figure 3, from number 7 in the north to number 1 in the south, indicates that the tip of the asthenospheric wedge between the downgoing and overriding plates progressively propagates upward and trenchward toward the south. In section 2 that crosses the trench at its deepest point, the Challenger Deep, this is most extreme. At that point, the forearc narrows to only ~50 km, and the distance from the actively spreading Mariana Trough back arc basin, which must be underlain by shallow asthenosphere, to the trench narrows to ~100 km. In between, a dispersed group of seamounts (at about 142.5°E 11.8°N, Figure 1a) appear to be the southward continuation of the magmatic arc [*Fryer*, 1996; *Fryer et al.*, 1998; *Martinez et al.*, 2000]. The crust of this newly developing magmatic arc may not have thickened a lot, but even if the crust is 10-km thick, the depth of about 2.0 km below sea level indicates that here too, only 50 km away from the trench, the asthenosphere is very shallow.

[18] This unique combination of unusually narrow plate-coupling zone in the Challenger Deep segment and shallow asthenosphere so close to the plate boundary helps explain why the Challenger Deep is the deepest point on the Earth's surface. We infer that these two factors combine beneath the southern Marianas to allow the subducting slab to dip more steeply in its shallowest segments and form the unusually deep trench. In the following section we discuss

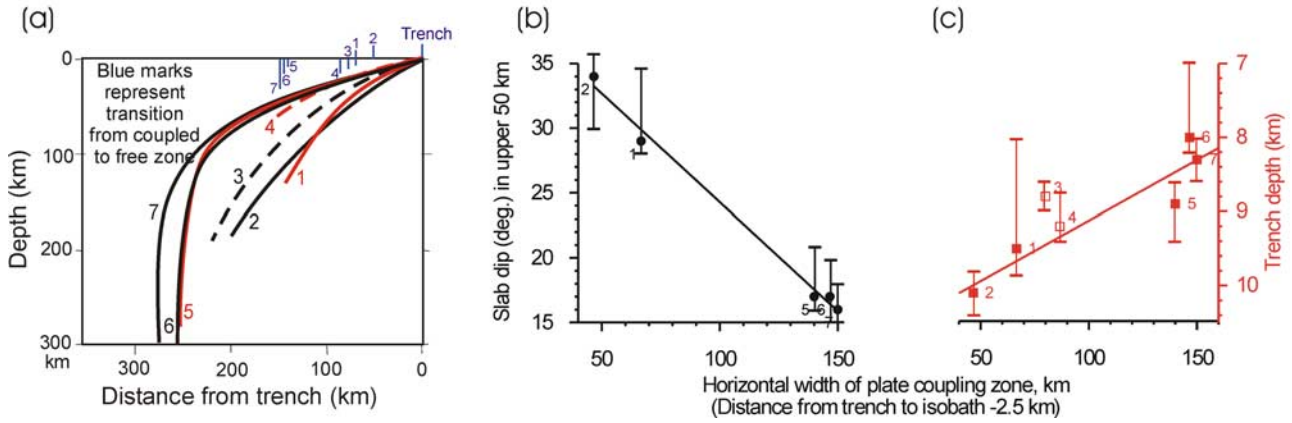

Figure 6. (a) A comparison between the tops of the subducting Pacific plate as inferred from the seven sections of Figure 3. The blue marks on the horizontal axis represent the transition from the coupled to the free zone. Note that the transition point is closer to the trench as the upper portion of the subducting plate steepens. (b) Correlation between the angle of subduction (dip of the top of the subducting plate) in the upper 50 km of downgoing plate and the width of plate-coupling zone. Width of the plate-coupling zone is measured from the trench to isobath −2.5 km, assuming that this is approximately the transition from the coupled to the free zone (point B in Figure 4). Black points represent the dip angle of the solid lines in Figure 3. Error bars represent the difference between the dips of the upper and lower dashed lines. Sections 3 and 4 in the disrupted area SW of Guam are not shown, because slab dip cannot be measured there (see Figures 3, 8a, and 8b). (c) Correlation between trench depth and the width of plate-coupling zone. Rectangles represent trench depth averaged along the ~100-km segment marked on Figure 1a. The large depth variations within each segment (see also Figure 2) are shown by vertical bars. Sections 3 and 4 are displayed as empty rectangles, but not included in the linear regression, because these sections are located in a disturbed area.

why this has happened at the southern end of the Marianas and not elsewhere.

5. Discussion

5.1. Slab Dip, Trench Depth, and the Width of the Pulled-Down Zone

[19] We have found a correlation between (1) deepening of the Mariana Trench; (2) shallowing of the Mariana Ridge; (3) steepening of the subducting Pacific plate at the upper 50–100 km; (4) narrowing of the plate-coupling zone; and (5) upward and trenchward propagation of asthenosphere between the downgoing and overriding plates. The correlation between trench depth and slab dip has been shown previously [*Jarrard*, 1986], however, the dependence of these two parameters on the width of the plate-coupling zone, as shown in Figure 6, is a new contribution of this study. We propose that the southward weakening of plate coupling frees the two plates from one another, allowing the descending plate to steepen and form a deeper trench and at the same time allowing the edge of the upper plate to rebound and form a shallower ridge. The absence of a shallowing trend along the West Mariana Ridge (blue line in Figure 4) away from the plate boundary reinforces this argument.

5.2. Plate Coupling and Slab Dynamics

[20] The difference between the present geometry of the shallow subduction zone in the central and southern Marianas still does not explain why the 200-km-long slab in section 2 has almost detached from the overriding plate, while the 700+-km-long slab in section 7 is still associated with a broad coupling zone. What is the difference between central and southern Marianas and what is so special in the Challenger Deep segment?

[21] In our opinion the special situation at the southernmost Marianas results from active steepening of the subducting slab that produces an angular moment that overcomes plate coupling (Figure 7). This conclusion is, first, based on theoretical considerations. The exceptionally shallow asthenospheric penetration between the subducting and overriding plates (section 2 of Figures 3 and 7b) is not thermally stable and cannot remain for long [*Gvirtzman and Nur*, 1999b]. Its existence, therefore, indicates that this process is both active and rapid.

[22] In addition, field evidence supporting active slab steepening beneath the southernmost Marianas was suggested by *Fryer et al.* [2003, 2001] from side-scan sonar images that reveal numerous normal faults in the forearc west of Guam. According to these authors forearc extension in this region is caused by vigorous slab rollback and trench retreat. They also argue that the lack of sediments covering the deformed ocean floor further indicates that the accelerated extension and southward migration of the Mariana Trench in this region has occurred recently. One may argue that extensional faulting of forearcs alone is not enough to prove slab rollback, because normal faulting may also be caused by basal subduction erosion, but we

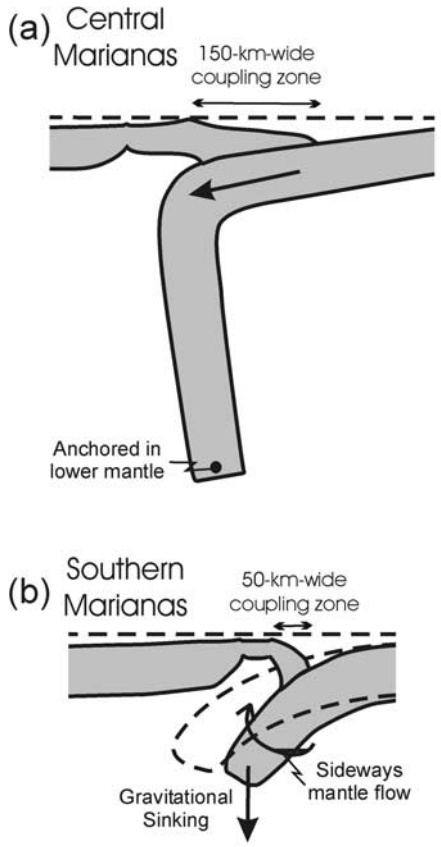

Figure 7. A cartoon illustrating the difference between the subduction zone beneath the central and southern Marianas. (a) The slab beneath the central Marianas is strongly bent, because of the lateral forces operating on its top and bottom. Its top is pushed aside along with the Pacific plate, while its bottom is anchored in the lower mantle. The strong bending at 100–200-km depth separates a lower nearly vertical portion and an upper relatively flat portion. The flat upper portion is attached to the overriding plate along a 150-km-wide area and its gentle, near-surface, slope avoids further trench deepening. (b) The relatively short slab in the southernmost Marianas is rapidly steepening, but here the driving force is different. The hydrodynamic shape of the small slab here allows it to sink in the mantle by its own weight with minimal resistance from the mantle that can easily flow around its edges. This rapid steepening is producing an angular moment that overcomes plate coupling. As a result, the coupling zone is only about 50 km, the asthenosphere penetrates between the overriding and subducting plates almost up to the trench, and the steep subduction angle forms the deepest trench in the world.

still favor the rollback interpretation based on two additional lines of evidence: the shallow asthenosphere penetration between the two plates (this study) and the opening rate of the Mariana Trough back arc basin that increases southward [*Ishihara et al.*, 2001; *Kato et al.*, 2003; *Martinez et al.*, 2000]. These three processes are all explained by rapid rollback of the subducting slab.

[23] Note that *Fryer et al.* [1998, 2001, 2003] use the terms "slab rollback" and "trench retreat," which express the direction of motion relative to the overriding plate, whereas we use "slab steepening" with no directional meaning. We chose so, because of the absolute northwest motion of the Pacific plate, i.e., relative to the mantle, the Mariana Trench is advancing; not retreating (the cause for back arc opening in the Mariana Trough is the even faster northwest motion of the Philippine plate [*Sella et al.*, 2002]).

[24] The motion relative to the mantle is important for understanding slab dynamics beneath the central Marianas, where the slab extends down to more than 1000 km [*Van der Hilst et al.*, 1991] as detected by seismic tomography (~700 km is the length of the seismically active zone). In this case the northwestward motion of the upper portion of the slab along with the Pacific plate, and at the same time the anchoring of its deep tip in the lower mantle, causes it to bend (Figure 7a). As a result, the upper portion of the slab above the bending zone (depths of 100–200 km) is relatively flat, whereas its lower portion is very steep (sections 6–7). On the basis of our analysis, which reveals a wide coupling zone between the shallow flat portion of the slab and the overriding plate, we suggest that this flat position is quite stable now. We further suggest that this stability is not only maintained by the resistance of the plates to detach from one another, but also by the resistance of the lower mantle to the vertical sinking of the entire slab.

5.3. What Has Triggered Rapid Slab Steepening in the Southernmost Marianas?

[25] Steepening (or rollback) of the subducted plate beneath the southernmost Marianas is very different from the process described above. In this case the lateral forces operating on the slab are not as strong, first, because of the oblique direction of subduction (that is, the resistance of the mantle to the northwestward advancing slab is weaker than in the central Marianas); and, second, because the short slab does not reach the lower mantle and its tip is not anchored anywhere. So, if lateral forces are not the major cause for slab steepening beneath the southernmost Marianas, what is the cause for its rapid steepening? In our opinion, slab motion here is driven by simple gravitational sinking; the special situation created here is not related to the slab's load, but to its hydrodynamic shape.

[26] It has already been demonstrated that narrow, hydrodynamically shaped slab fragments can easily move in the mantle, because the sideways mantle flow around their edges reduces the resistance of the mantle to their motion [*Dvorkin et al.*, 1993; *Nur et al.*, 1991]. It has also been demonstrated that steepening slabs minimize their attachment to the overriding plates and allow the overriding plates to rebound [*Gvirtzman*, 2002; *Gvirtzman and Nur*, 1999a, 1999b, 2001]. Consistent with this approach we suggest that a similar process takes place here at the southernmost edge of the Mariana subduction zone, where the subducting Pacific plate steepens where sideways mantle flow is possible.

[27] Furthermore, we suspect that in addition to the proximity to the edge, the lithosphere subducting beneath

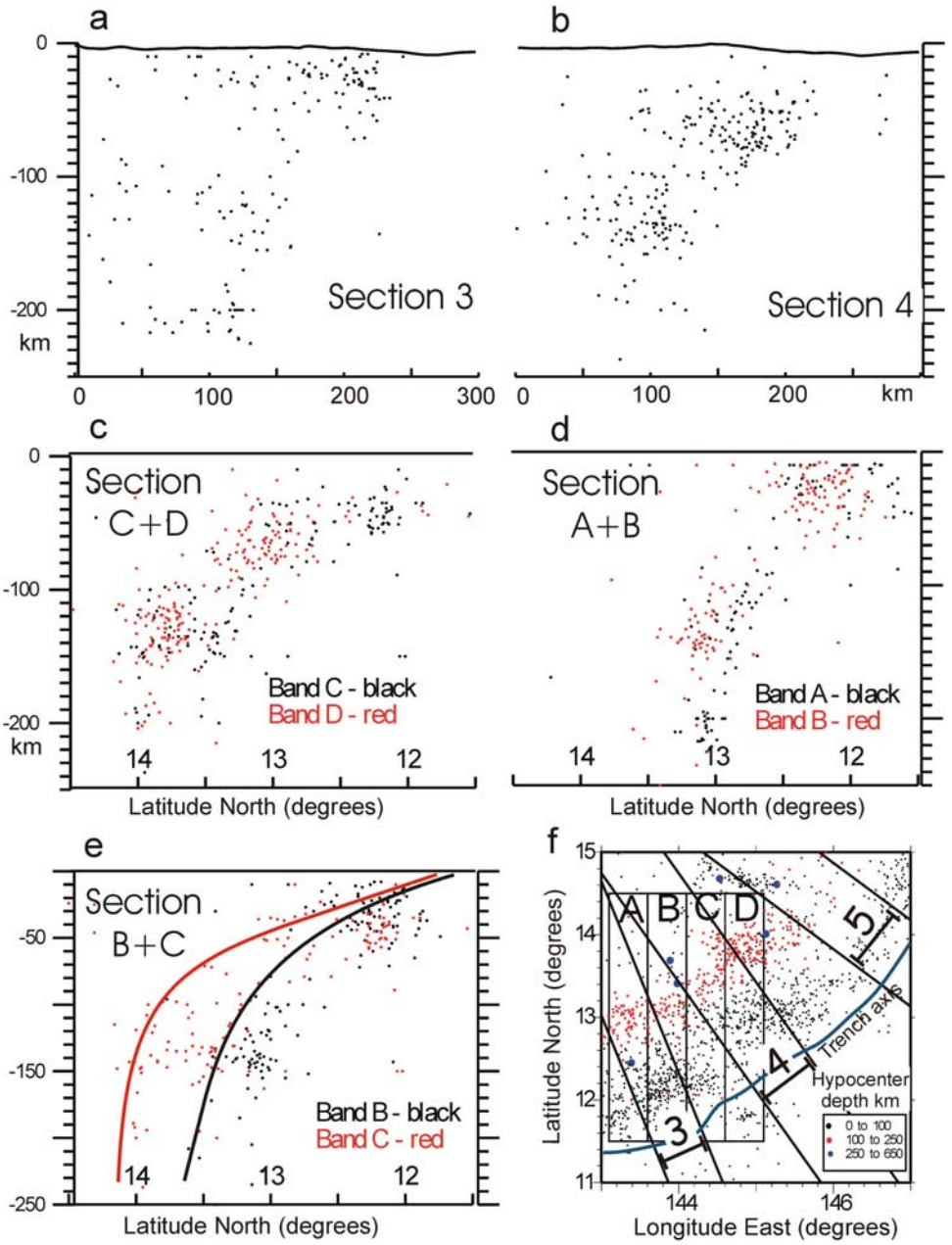

Figure 8. Evidence for a slab tear SW of Guam. (a and b) Exceptionally wide seismic zone in sections 3 and 4 showing a disturbed Wadati-Benioff Zone. (c and d) Northward trending sections along slices A, B, C, and D (locations in Figure 8f) with a relatively "normal" seismic zone indicating that the slab here probably dips northward. In addition, hypocenters from slices C and D together (c) and from slices A and B together (d) produce a homogenous distribution of epicenters, whereas B and C together produce a bimodal distribution of earthquakes (e). This bimodal distribution suggests that the slab between sections B and C is torn into two separate pieces with different dip angles. (f) Map of earthquake epicenters showing that the inferred slab tear at approximately 144.1°E coincides with a noticeable disruption of the red points representing epicenters within the depth interval of 100–250 km.

the Challenger Deep segment is now tearing away from the rest of the plate. This releases a small slab fragment allowing it to independently roll back toward the south and steepen more easily. Indications for a possible tear in the subducting plate come from the seismicity pattern southwest of Guam (sections 3 and 4 of Figures 3 and 8), which reveal an exceptionally diffuse seismic zone. This suggests that the Wadati-Benioff Zone beneath this region is disrupted and

that the dip of the slab may not be perpendicular to the general curvature of the trench. In contrast, north-trending sections crossing the same area (Figures 8c and 8d) show a typical seismic zone, suggesting that the true dip of the subducting slab here is almost north. Of particular importance is the division of the disrupted area to four N-S bands labeled A-D in the map of Figure 8f. Figure 8d shows that the earthquakes from bands A (black points) and B (red points) together produce an homogenous mix of points composing a typical Wadati-Benioff Zone. Similarly, the earthquakes from bands C (black points) and D (red points) together also show a typical Wadati-Benioff Zone (Figure 8c). However, the points from B (black) and C (red) together produce a bimodal distribution of earthquakes, suggesting two different dip angles (the black and red lines of Figure 8e). We infer that these two angles represent two separate pieces of lithosphere on the two sides of a slab tear located between bands B and C, that is along longitude 144.1°E. This inferred tear (marked on Figure 1a by a thick white line and illustrated in the cartoon of Figure 9) coincides with three other observations: (1) it separates two clusters of red points in the Earthquake epicenter map (Figure 8f), (2) it coincides with the sharp termination of the Mariana Ridge immediately southwest of Guam [*Fryer*, 1996; *Fryer et al.*, 1998; *Martinez et al.*, 2000] (Figure 1a); and (3) it coincides with a set of large, north striking, left-lateral, strike-slip faults, recently mapped and interpreted by *Fryer et al.* [2001, 2003] as the surface expression of a slab tear.

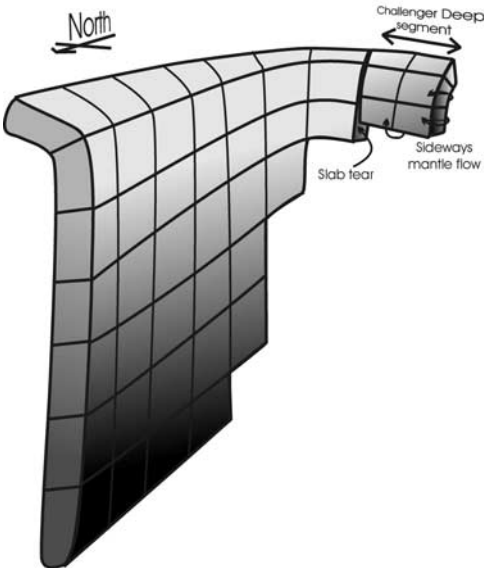

Figure 9. Cartoon illustrating the shape of the lithosphere subducting beneath central and southern Marianas. The small slab fragment beneath the Challenger Deep segment is released from the rest of the subducting plate to independently steepen as mantle material flows around it. Note that the upper flat portion of the slab that is strongly coupled to the overriding plate pulling the forearc region downward narrows southward.

5.4. Recent Reorganization of Subduction Near the Challenger Deep Segment

[28] The great length of the subducted slab north of Guam reflects 45 million years of subduction (a mean subduction rate of 3 cm/yr generates a 1350-km-long slab, about what is observed), whereas the much shorter slab associated with the Challenger Deep segment implies a much more youthful onset of subduction (a 200-km-long slab can be generated in 7 Ma at 3 cm/yr). This relatively young onset of subduction in the south approximately coincides with the opening of the Mariana Trough back arc basin with rifting beginning sometime after 10 Ma and seafloor spreading beginning about 3–4 Ma [*Stern et al.*, 2003]. Moreover, the wide and rapid opening in the south is coupled with lengthening of the Challenger Deep segment in the E-W direction. All together, these processes require the subduction zone to continuously reorganize. One consequence of this reorganization is the tearing of the subducted plate at the transition zone, where the trench-arc system changes its strike from N-S to nearly E-W (Figure 9). As explained above, this tearing enhances the steepening of the slab beneath the Challenger Deep segment, which is responsible for the formation of the deepest point on the Earth's surface.

5.5. Topography, Isostasy, and Gravity

[29] In general, isostasy or the lack of it is expressed by topography as well as by gravity, but here we distinguish between the two. We assume that in the Free Floating Zone the topography is not influenced by the subducting plate, because the low viscosity of the asthenosphere effectively separates the subducting and overriding plates and does not transmit significant forces from the descending slab upward. In contrast, the gravity signal generated by the subducting lithosphere is felt at the surface regardless of the asthenosphere wedge between the plates. A nice analogue for this situation is a boat floating over a huge stone that lies on the bottom of the lake [*Sleep and Fujita*, 1997]. The excess mass of the stone does not influence of the floating conditions of the boat, but it surely does influence the gravity field.

[30] This explanation is good for the positive long-wavelength (hundreds of kilometers) signal on the order of a few tens of milligals produced by the excess mass of the subducting lithosphere (Figure 10a) [see also *Watts and Talawani*, 1975]. However, what is the cause for the stronger, short-wavelength, free air anomalies in the arc/back arc region? These anomalies, which are caused by lateral variations in topography and crustal thickness, also do not indicate the lack of isostatic equilibrium. They only indicate edge effects of relatively narrow topographic elements as illustrated in Figure 10b. For example, the excess mass of the left ridge in Figure 10b produces a positive signal; its crustal root produces a wider and weaker negative signal; and the net effect is a wave-shaped anomaly, about plus 130 mGals in the center and about minus 30 mGals on the margins. Such anomalies are observed at the margins of wide mountain ranges, which are surely compensated by their roots, as evident by the nearly zero free air anomaly in their central region, where the positive and negative signals cancel each other. Here

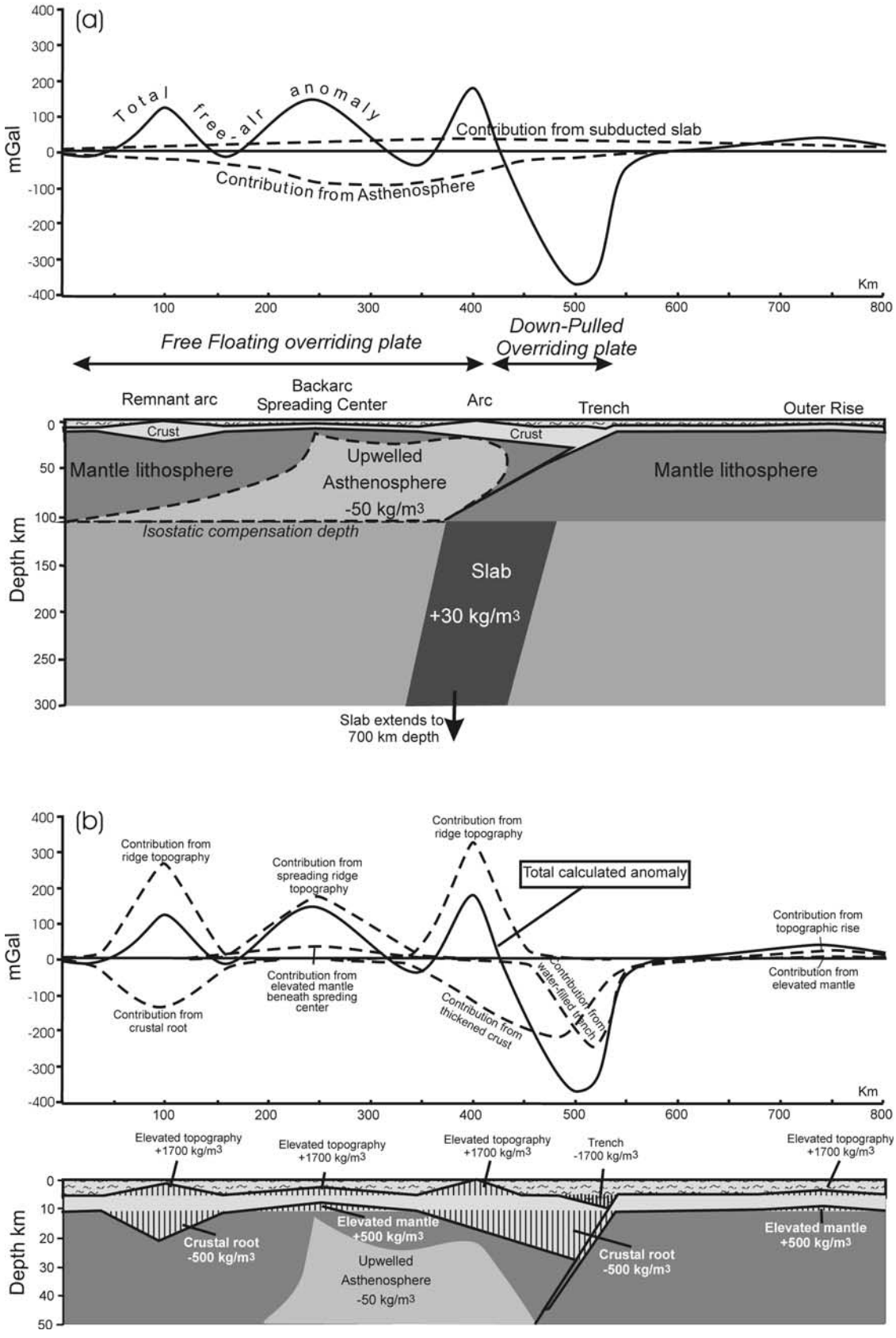
(a)
Total free-air anomaly
Contribution from subducted slab
Contribution from Asthenosphere
mGal
Km
Free Floating overriding plate
Down-Pulled Overriding plate
Remnant arc
Backarc Spreading Center
Arc
Trench
Outer Rise
Crust
Crust
Mantle lithosphere
Upwelled Asthenosphere -50 kg/m3
Mantle lithosphere
Isostatic compensation depth
Slab +30 kg/m3
Depth km
Slab extends to 700 km depth
(b)
Contribution from ridge topography
Contribution from spreading ridge topography
Contribution from ridge topography
Total calculated anomaly
Contribution from topographic rise
Contribution from elevated mantle
Contribution from elevated mantle beneath spreding center
Contribution from crustal root
Contribution from thickened crust
Contribution from water-filled trench
mGal
Km
Elevated topography +1700 kg/m3
Elevated topography +1700 kg/m3
Elevated topography +1700 kg/m3
Trench -1700 kg/m3
Elevated topography +1700 kg/m3
Crustal root -500 kg/m3
Elevated mantle +500 kg/m3
Upwelled Asthenosphere -50 kg/m3
Crustal root -500 kg/m3
Elevated mantle +500 kg/m3
Depth km

Figure 10.

the entire ridge area is within the edge effect, but this does not indicate a lack of local compensation.

[31] In addition to the ridges, Figure 10b also shows that the elevated crust of the back arc spreading center generates a positive signal of more than 100 mGals, and that this signal is only partly compensated by the much wider and a bit weaker negative signal generated by the upwelling asthenosphere (about −80 mGals; Figure 10b). Together, the ridges, the spreading center, and the deep-seated slab produce a positive free air anomaly with short-wavelength variations.

[32] Though this presentation of gravity in a Mariana-type subduction zone is simplified, it serves to explain why we can assume isostatic equilibrium in the arc-back arc region in spite of the free air gravity anomalies observed there. The short-wavelength edge effects do not indicate a lack of isostatic compensation; whereas the long- wavelength positive signal of the deep slab has nothing to do with the internal mass distribution in the crust and mantle above it. On the contrary, if the asthenosphere has a low enough viscosity to maintain hydrostatic pressure, as assumed by the isostatic theory, then all rock columns above a certain compensation depth within the asthenosphere must have the same cumulative mass. Within each of these columns excess masses are compensated by density deficits and vice versa and this is what allows our calculations.

[33] Finally, Figure 10 helps explain why we have not used gravity data to identify the transition between the Pulled-Down and Free Floating zones. This would require locating the tip of the asthenospheric wedge from gravity data. However, considering the very weak negative signal of the asthenosphere compared to the much stronger negative signal of the thick crust under the arc and forearc, one can imagine that this effort is almost impossible. In contrast, the expression of the transition from Pulled-Down to Free Floating zones is evident in the topography as shown above.

6. Conclusion

[34] We suggest that tearing of the subducting Pacific plate and the upwelling of asthenosphere beneath the southernmost Mariana Trough combine to allow the southernmost fragment of the subducting lithosphere to independently roll back, reduce its coupling to the upper lithosphere, and steepen. This steepening results in an unusually deep trench that forms the deepest point on the Earth's solid surface (Figures 7 and 9). This is consistent with recent investigations that suggest the rate of seafloor spreading in the Mariana Trough increases southward [*Ishihara et al.*, 2001; *Kato et al.*, 2003; *Martinez et al.*, 2000].

[35] In a wider perspective, the difference between central and southernmost Marianas demonstrates the relative importance of several factors controlling slab dynamics. Beneath the central Marianas the subducting slab is very long and heavy. The vertical load it produces is, thus, very large. On the other hand, three other factors resist its vertical sinking. Its lower tip has difficulty to sink in the more viscous lower mantle; its upper portion is strongly attached to the overriding plate; and its wide extent in the N-S direction does not provide a hydrodynamic shape and resists vertical sinking in the mantle.

[36] However, in spite of its difficulty to sink vertically, the slab beneath central Marianas has steepened to a nearly vertical position, because of the opposite lateral forces operating on its top and bottom. Its upper portion moves northwestward along with the Pacific plate while its tip is anchored in the lower mantle. Right now the movement steepening lower portion of the slab is separated from its upper portion by a strong bending point.

[37] The southernmost Marianas, on the other hand, are an excellent example for vertical sinking of a hydrodynamically shaped slab fragment (Figure 9). The slab beneath the Challenger Deep segment is shorter and younger than the slab beneath central Marianas, and thus the vertical load it generates is much smaller. However, its excellent hydrodynamic shape reduces mantle resistance and allows it to retreat and steepen by its own weight. All of this is ultimately a response to the opening of the southernmost Mariana Trough. Thus, the great depth of the Challenger Deep is due to a narrow subducting slab that formed as the lower plate responds to extension in the upper plate.

Appendix A: Crustal Versus Mantle Contributions to Topography

[38] The mean elevation, ε, of a region that is in isostatic equilibrium can be considered as a sum of contributions from the buoyancy of the crust (H_c) and from the buoyancy

Figure 10. Calculated gravity for a simplified Mariana-type subduction zone. (a) Contributions of mantle inhomogeneities to gravity. The total calculated free air anomaly (solid line) is shown relative to the individual contributions of the upwelled asthenosphere and the subducted slab (dashed lines). Density contrasts are 50 kg/m^3 between asthenosphere and the surrounding mantle lithosphere and 30 kg/m^3 between the cold slab and its surrounding mantle material (changing these values by 10–50 kg/m^3 does not change the general nature of these weak and long wavelength anomalies [*Watts and Talawani*, 1975]). (b) Contribution of crustal inhomogeneities to gravity. The total calculated free air anomaly (solid line) is compared to the short-wavelength individual contributions (dashed lines) of topographic ridges, thickened crust, water-filled trench, back arc spreading ridge, and seaward outer rise. Density contrasts are 1700 kg/m^3 between crust and water and 500 kg/m^3 between crust and mantle. This modeling illustrates that most of the free air gravity anomaly across the arc is attributed to edge effects of relatively narrow structural elements (see text). This does not indicate that the excess mass of ocean floor topography is not locally compensated by density deficits below it. On the contrary, if the asthenosphere has a low enough viscosity to maintain hydrostatic pressure, as assumed by the isostatic theory, then all rock columns above the marked compensation depth must have the same cumulative mass. Within each of these columns excess masses are compensated by density deficits and vice versa regardless of the mass distribution below them.

of the mantle lithosphere (H_{ml}). *Lachenbruch and Morgan* [1990] have shown that

$$\varepsilon = a(H_c + H_{ml} - H_0) \qquad \begin{array}{ll} a = 1 & \varepsilon \geq 0 \\ a = \dfrac{\rho_a}{\rho_a - \rho_w} & \varepsilon < 0 \end{array} \tag{A1}$$

where ρ_a and ρ_w are the densities of the asthenosphere and water, respectively; a expresses the effect of deepening of ocean floor due to the load of the water ($a \approx 1.45$); and H_0 is a constant that allows the use of sea level as a reference datum. *Lachenbruch and Morgan* [1990] have further shown that a value $H_0 \approx 2.4$ km makes equation (A1) consistent with the density and elevations of mid-ocean ridges.

[39] In this formulation, H_c and H_{ml} are defined as follows:

$$H_c = \frac{1}{\rho_a}(\rho_a - \rho_c)L_c \tag{A2}$$

$$H_{ml} = \frac{1}{\rho_a}(\rho_a - \rho_{ml})L_{ml}, \tag{A3}$$

where ρ_c and L_c are the density and the thickness of the crust, respectively, and ρ_{ml} and L_{ml} are the density and the thickness of the mantle lithosphere.

[40] In reality, it is easier to estimate H_c than to estimate H_{ml}, specifically where the seismic velocity structure of the crust is known, and thus the data constrain the thickness and density of the crust much better than the thickness and density of the mantle lithosphere. In general, it is worth remembering that H_c is always positive because the crust is lighter then the asthenosphere, whereas H_{ml} is always negative because the mantle lithosphere is heavier than the asthenosphere (same composition but cooler).

[41] If we assume that residual variations in the Earth's topography that are not explained by variations in the buoyancy of the crust are attributed to variations in the buoyancy of the mantle [*Jones et al.*, 1992; *Lachenbruch and Morgan*, 1990; *Mooney et al.*, 1998], we can calculate H_{ml} from equation (A1):

$$H_{ml} = \frac{\varepsilon}{a} + H_0 - H_c. \tag{A4}$$

[42] If the average density of the mantle lithosphere is assumed or known, its thickness L_{ml} can be determined using equation (A3):

$$L_{ml} = \frac{\rho_a}{\rho_a - \rho_{ml}}\left(\frac{\varepsilon}{a} + H_0 - H_c\right). \tag{A5}$$

[43] Here we follow *Lachenbruch and Morgan* [1990] and *Jones et al.* [1992], who used $\rho_a = 3200$ kg/m^3 and $\rho_{ml} = 3250$ kg/m^3. The significance of choosing a different density for the mantle lithosphere is discussed by *Gvirtzman and Nur* [2001].

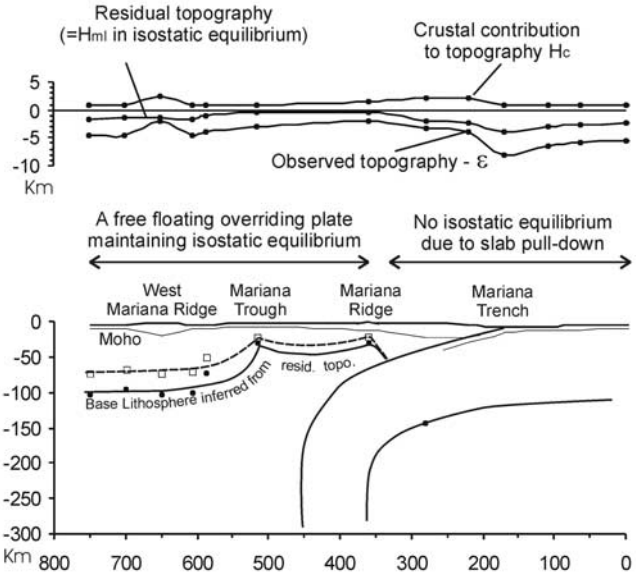

Figure A1. A detailed application of the topography analysis [*Gvirtzman*, 2002; *Gvirtzman and Nur*, 1999a, 1999b, 2001] along section 7 (details in Appendix A). This analysis infers plate thickness assuming that if isostatic equilibrium is maintained, the observed topography, ε, is actually the sum of the contribution from the buoyancy of the crust (H_c) and a contribution from the buoyancy of the mantle lithosphere (H_{ml}). Therefore, with a given crustal structure, the thickness of the mantle lithosphere can be calculated in a way that matches the total buoyancy of the lithosphere with the observed surface elevation. The upper set of curves show the various stages of the analysis. First, H_c is calculated and removed from the observed surface elevation, ε. Then, the residual topography is examined from the trench arcward, and the transition point from where the residual topography is no longer lower than expected from the local lithospheric column is identified (point B here as in Figure 4). From that point onward it is assumed that the overriding plate is free and maintains local isostatic equilibrium and, therefore, the residual topography is, in fact, the contribution of the mantle lithosphere, H_{ml}. Finally, using 3250 kg/m^3 and 3200 kg/m^3, as average densities for the mantle-lithosphere and asthenosphere, respectively, H_{ml} is transformed into mantle-lithosphere thickness and the base of the overriding plate is inferred. The dashed line shows the calculated base of the lithosphere if 3270 kg/m^3 is chosen as the average density of the mantle-lithosphere. This value corresponds to defining the base of the lithosphere as the 1100°C isotherm instead of 1350°C [*Gvirtzman and Nur*, 2001]. Note that the topography, ε, is always lower than H_c, because the mantle-lithosphere, which is generally heavier than the asthenosphere (negative H_{ml}), pulls the crust downward to a position lower than expected from its own buoyancy alone (see discussion about the uncertainties of this method from *Gvirtzman and Nur* [2001]).

[44] Figure A1 illustrated how the topography analysis is carried out step by step using section 7 along 18°N as an example (crustal structure after *Fryer and Hussong* [1981]). First, the theoretical contribution of crust to the topography, H_c, is calculated and removed from the observed surface elevation, ε. Then, the residual topography is examined from the trench arcward and the transition point where the residual topography is no longer lower than expected from the local lithospheric column is identified (point B in Figure 2, approximately at water depth of −2.5 km). West of that point, it is assumed that the overriding plate is free and maintains local isostatic equilibrium, and therefore residual topography can be used as a proxy for the contribution of the mantle lithosphere, H_{ml}. Using 3250 kg/m^3 and 3200 kg/m^3 as average densities for mantle-lithosphere and asthenosphere, respectively, the mantle-lithosphere contribution to the topography is transformed into mantle-lithosphere thickness and the base of the overriding plate is inferred. The dashed line in Figure A1 shows the calculated base of the lithosphere if 3270 kg/m^3 is chosen as the average density of the mantle-lithosphere. The values of 3250 kg/m^3 and 3270 kg/m^3 correspond to different definitions for the base of the lithosphere: 1350°C and 1100°C isotherms, respectively [*Gvirtzman and Nur*, 2001]. Note that the mantle-lithosphere contribution is always negative, because the mantle-lithosphere is heavier on average that the asthenosphere (uncertainties related to this method are discussed by *Gvirtzman and Nur* [2001]).

[45] **Acknowledgments.** We would like to express our gratitude to Serge Lallemand and Susan Buiter for their constructive and helpful reviews. We also thank Dave Scholl for his detailed and most helpful remarks on an early version of this study.

References

Bibee, L. D., M. Reichle, and R. M. Keickhefer (1979), Seismic structure of the West Mariana ridge, *Eos*, *60*, 950.

Dvorkin, J., A. Nur, G. Mavko, and Z. Ben Avraham (1993), Narrow subducting slabs and the origin of backarc basins, *Tectonophysics*, *227*, 63–79.

Fryer, P. (1996), Evolution of the Mariana convergent plate margin system, *Rev. Geophys.*, *34*, 89–125.

Fryer, P., and D. M. Hussong (1981), Seafloor spreading in the Mariana Trough: Results of Leg 60 drill site selection, *Initial Rep. Deep Sea Drill. Proj.*, *60*, 45–65.

Fryer, P., H. Fujimoto, M. Sekine, L. E. Johnson, J. Kasahara, H. Masuda, T. Gamo, T. Ishii, M. Ariyoshi, and K. Fujioka (1998), Volcanoes of the southwestern extension of the active Mariana island arc: New swath-mapping and geochemical studies, *Island Arc*, *7*, 596–607.

Fryer, P., F. Martinez, N. Becker, B. Appelgate, J. Hawkins, and T. Ishihara (2001), A subduction factory laboratory: Tectonics of the southern Mariana convergent margin, *Eos*, *82*, 1187.

Fryer, P., N. Becker, B. Appelgate, F. Martinez, M. Edwards, and G. Fryer (2003), Why is the Challenger Deep so deep?, *Earth Planet. Sci. Lett.*, *211*, 259–269.

Fujioka, K., K. Okino, T. Kanamatsu, and Y. Ohara (2002), Morphology and origin of the Challenger Deep in the Southern Mariana Trench, *Geophys. Res. Lett.*, *29*(10), 1372, doi:10.1029/2001GL013595.

Grellet, C., and J. Dubois (1982), The depth of trench as a function of the subduction rate and age of the lithosphere, *Tectonophysics*, *82*, 45–56.

Gudmundsson, O., and M. Sambridge (1998), A regionalized upper mantle (RUM) seismic model, *J. Geophys. Res.*, *103*, 7121–7136.

Gvirtzman, Z. (2002), Partial detachment of a lithospheric root under the Southeast Carpathians: Toward a better definition of the detachment concept, *Geology*, *30*, 51–54.

Gvirtzman, Z., and A. Nur (1999a), The formation of Mount Etna as the consequence of slab rollback, *Nature*, *401*, 782–785.

Gvirtzman, Z., and A. Nur (1999b), Plate detachment, asthenosphere upwelling, and topography across subduction zones, *Geology*, *27*, 563–566.

Gvirtzman, Z., and A. Nur (2001), Lithospheric structure and sunken slabs in the central Mediterranean, *Earth Planet. Sci. Lett.*, *187*, 117–130.

Ishihara, T., R. J. Stern, P. Fryer, S. H. Bloomer, and N. C. Becker (2001), Seafloor spreading in the southern Mariana trough inferred from 3-component magnetometer data, *Eos*, *82*(47), Fall Meet. Suppl., Abstract T41C-0895.

Jarrard, R. D. (1986), Relation among subduction parameters, *Rev. Geophys.*, *24*, 217–284.

Jones, H. J., B. P. Wernicke, G. L. Farmer, J. D. Walker, D. S. Coleman, L. W. McKenna, and F. V. Perry (1992), Variations across and along a major continental rift: An interdisciplinary study of the Basin and Range Province, western USA, *Tectonophysics*, *213*, 57–96.

Karig, D. E., and B. Rankin (1983), Marine geology of the forearc region, southern Mariana Island arc, in *The Tectonic and Geologic Evolution of Southeast Asian Seas and Islands: Part 2*, *Geophys. Monogr. Ser.*, vol. 27, edited by D. E. Hayes, pp. 266–280, AGU, Washington, D. C.

Kato, T., J. Beavan, T. Matsushima, Y. Kotake, J. Camacho, T. Jaun, and S. Nakao (2003), Geodetic evidence of backarc spreading in the Mariana Trough, *Geophys. Res. Lett.*, *30*, 1625, doi:10.1029/2002GL016757.

Lachenbruch, A. H., and P. Morgan (1990), Continental extension, magmatism and elevation: Formal relations and rules of thumb, *Tectonophysics*, *174*, 39–62.

Lange, K. (1992), Auswertung eines weitwinkelreflexions und refraktionsseismischen profiles im suedlichen Marianen backarc becken, Diplomarbeit, Univ. Hamburg, Hamburg, Germany.

Latraille, S. L., and D. M. Hussong (1980), Crustal structure across the Mariana island arc, in *The Tectonic and Geologic Evolution of Southeast Asian Seas and Islands*, *Geophys. Monogr. Ser.*, vol. 23, edited by D. E. Hayes, pp. 209–221, AGU, Washington, D. C.

Martinez, F., P. Fryer, and N. Becker (2000), Geophysical characteristics of the southern Mariana Trough, 11°50′N–13°40′N, *J. Geophys. Res.*, *105*, 16,591–16,607.

Mooney, W. D., G. Lask, and T. G. Master (1998), CRUST 5.1: A global crustal model at 5° × 5°, *J. Geophys. Res.*, *103*, 727–747.

Nur, A., J. Dvorkin, G. Mavko, and Z. Ben Avraham (1991), Speculations on the origin and fate of backarc basins, *Ann. Geofis.*, *36*, 155–163.

Pacheco, J., L. Sykes, and C. Scholz (1993), Nature of seismic coupling along simple plate boundaries of the subduction types, *J. Geophys. Res.*, *98*, 14,133–14,159.

Peterson, E. T., and T. Seno (1984), Factors affecting seismic moment release rates in subduction zones, *J. Geophys. Res.*, *89*, 10,233–10,248.

Ruff, L. J., and H. Kanamori (1980), Seismicity and subduction process, *Phys. Earth Planet. Inter.*, *23*, 240–252.

Scholz, C. H., and J. Campos (1995), On the mechanism of seismic decoupling and backarc spreading at subduction zones, *J. Geophys. Res.*, *100*, 2103–2115.

Sella, G. F., T. H. Dixon, and A. Mao (2002), REVEL: A model for Recent plate velocities from space geodesy, *J. Geophys. Res.*, *107*(B4), 2081, doi:10.1029/2000JB000033.

Seno, T., S. Stein, and A. Gripp (1993), A model for the motion of the Philippine Sea Plate consistent with NUVEL-1 and geological data, *J. Geophys. Res.*, *98*, 17,941–17,948.

Sleep, N. H., and K. Fujita (1997), *Principles of Geophysics*, 608 pp., Blackwell, Malden, Mass.

Stern, R. J., M. J. Fouch, and S. Klemperer (2003), An overview of the Izu-Bonin-Mariana subduction factory, in *Inside the Subduction Factory*, *Geophys. Monogr. Ser.*, vol. 138, edited by J. Eiler and M. Hirschmann, pp. 175–222, AGU, Washington, D. C.

Van der Hilst, R. D., E. R. Engdahl, W. Spakman, and G. Nolet (1991), Tomographic imaging of subducted lithosphere below northwest Pacific island arcs, *Nature*, *353*, 37–43.

Watts, A. B., and M. Talawani (1975), Gravity effect of downgoing lithospheric slab beneath island arcs, *Geol. Soc. Am. Bull.*, *86*, 1–4.

Zhang, J., and C. A. Langston (1995), Constraints on oceanic lithosphere structure from deep-focus regional receiver function inversions, *J. Geophys. Res.*, *100*, 2187–2196.

Z. Gvirtzman, Geological Survey of Israel, 30 Malkhei Yisrael Street, Jerusalem, 95501, Israel. (zohar@mail.gsi.gov.il)

R. J. Stern, Geosciences Department, University of Texas at Dallas, Box 830688, Richardson, TX 75083-0688, USA. (rjstern@utdallas.edu)